ANESTHESIOLOGY

End-tidal to Arterial Gradients and Alveolar Deadspace for Anesthetic Agents

Philip J. Peyton, M.D., Ph.D., M.B.B.S., F.A.N.Z.C.A., Jan Hendrickx, M.D., Ph.D., Rene J. E. Grouls, Pharm.D., Ph.D., Andre Van Zundert, M.D., Ph.D., F.R.C.A., E.D.R.A., F.A.N.Z.C.A., Andre De Wolf, M.D.

ANESTHESIOLOGY 2020; 133:534–47

EDITOR'S PERSPECTIVE

What We Already Know about This Topic

- General anesthesia increases the inhomogeneity (scatter) of the distribution of ventilation-perfusion ratios in the lung, widening alveolar to arterial partial pressure gradients for respired gases
- This inhomogeneity is reflected in increased alveolar deadspace fraction in the traditional three-compartment model of ventilation-perfusion scatter
- The alveolar to arterial partial pressure difference for isoflurane is inconsistent with that measured simultaneously using end-tidal and arterial carbon dioxide partial pressures

What This Article Tells Us That Is New

- Alveolar deadspace fraction calculated for volatile anesthetic agents is much larger than that calculated simultaneously for carbon dioxide, and its magnitude increases as blood solubility decreases
- Physiologically realistic multicompartment modeling of ventilation-perfusion scatter explains the relative differences between inhalational agents in alveolar to arterial partial pressure gradients and alveolar deadspace

ABSTRACT

Background: According to the "three-compartment" model of ventilation-perfusion ($\dot{V}_A/\dot{Q}$) inequality, increased $\dot{V}_A/\dot{Q}$ scatter in the lung under general anesthesia is reflected in increased alveolar deadspace fraction (V_{DA}/V_A) customarily measured using end-tidal to arterial (A-a) partial pressure gradients for carbon dioxide. A-a gradients for anesthetic agents such as isoflurane are also significant but have been shown to be inconsistent with those for carbon dioxide under the three-compartment theory. The authors hypothesized that three-compartment V_{DA}/V_A calculated using partial pressures of four inhalational agents (V_{DA}/V_{AG}) is different from that calculated using carbon dioxide (V_{DA}/V_{ACO_2}) measurements, but similar to predictions from multicompartment models of physiologically realistic "log-normal" $\dot{V}_A/\dot{Q}$ distributions.

Methods: In an observational study, inspired, end-tidal, arterial, and mixed venous partial pressures of halothane, isoflurane, sevoflurane, or desflurane were measured simultaneously with carbon dioxide in 52 cardiac surgery patients at two centers. V_{DA}/V_A was calculated from three-compartment model theory and compared for all gases. Ideal alveolar (P_{AG}) and end-capillary partial pressure (Pc'_G) of each agent, theoretically identical, were also calculated from end-tidal and arterial partial pressures adjusted for deadspace and venous admixture.

Results: Calculated V_{DA}/V_{AG} was larger (mean ± SD) for halothane (0.47 ± 0.08), isoflurane (0.55 ± 0.09), sevoflurane (0.61 ± 0.10), and desflurane (0.65 ± 0.07) than V_{DA}/V_{ACO_2} (0.23 ± 0.07 overall), increasing with lower blood solubility (slope [*Cis*], –0.096 [–0.133 to –0.059], $P < 0.001$). There was a significant difference between calculated ideal P_{AG} and Pc'_G median [interquartile range], P_{AG} 5.1 [3.7, 8.9] *versus* Pc'_G 4.0 [2.5, 6.2], $P = 0.011$, for all agents combined. The slope of the relationship to solubility was predicted by the log-normal lung model, but with a lower magnitude relative to calculated V_{DA}/V_{AG}.

Conclusions: Alveolar deadspace for anesthetic agents is much larger than for carbon dioxide and related to blood solubility. Unlike the three-compartment model, multicompartment $\dot{V}_A/\dot{Q}$ scatter models explain this from physiologically realistic gas uptake distributions, but suggest a residual factor other than solubility, potentially diffusion limitation, contributes to deadspace.

(ANESTHESIOLOGY 2020; 133:534–47)

GENERAL anesthesia significantly worsens inhomogeneity of the distribution of ventilation-perfusion ratios ($\dot{V}_A/\dot{Q}$ scatter) in the lung, widening alveolar (end-tidal) to arterial (A-a) partial pressure gradients for respired gases.[1–8] Using the traditional "three-compartment" (Riley) model of $\dot{V}_A/\dot{Q}$ scatter (fig. 1), this is reflected in increased alveolar deadspace fraction, representing the contribution of high $\dot{V}_A/\dot{Q}$ ratio lung regions to inefficiency of gas exchange, as well as an increase in venous admixture representing regions of low $\dot{V}_A/\dot{Q}$ ratio. While physiologic deadspace (V_D/V_T) is customarily measured from the Bohr–Enghoff equation using mixed expired and arterial carbon dioxide partial pressure measurements,[1,8] alveolar deadspace fraction (V_{DA}/V_A) can be calculated from the same mixing principle

This article is featured in "This Month in Anesthesiology," page 1A. This article has a video abstract. This article has a visual abstract available in the online version.

Submitted for publication January 31, 2020. Accepted for publication June 9, 2020. From the Anaesthesia, Perioperative and Pain Medicine Program, Centre for Integrated Critical Care, University of Melbourne, Melbourne, Australia (P.J.P.); the Department of Anaesthesia, Austin Health, Victoria, Australia (P.J.P.); the Institute for Breathing and Sleep, Victoria, Australia (P.J.P.); the Department of Basic and Applied Medical Sciences, Ghent University, Ghent, Belgium (J.H.); the Department of Anesthesiology, Onze-Lieve-Vrouw (OLV) Hospital, Aalst, Belgium (J.H.); the Department of Clinical Pharmacy, Catharina Hospital, Eindhoven, The Netherlands (R.J.E.G.); the Discipline of Anaesthesiology, Royal Brisbane and Women's Hospital, The University of Queensland, Brisbane, Australia (A.V.Z.); and the Department of Anesthesiology, Feinberg School of Medicine, Northwestern University, Chicago, Illinois (A.D.W.).

 Anesthesiology 2020; 133:534–47. DOI: 10.1097/ALN.0000000000003445

by measuring the end-tidal (P_{ETCO_2}) to arterial (P_{aCO_2}) carbon dioxide partial pressure gradient[9]

$$V_{DA} / V_A = 1 - P_{ETCO_2} / P_{aCO_2} \quad (1)$$

while the shunt equation of Berggren calculates venous admixture using blood oxygen content measurements (see appendix).[1,8] In this standard and familiar model, all gas exchange occurs in a theoretical "ideal compartment" of uniform $\dot{V}_A/\dot{Q}$ ratio where "ideal alveolar" and "pulmonary end-capillary" partial pressures for any gas *G* (ideal P_AG and $Pc'G$) are by definition identical.

In anesthetized patients, Landon *et al.*[9] confirmed the findings of previous authors that the A-a partial pressure difference for isoflurane was substantial, but also showed it to be inconsistent under three-compartment theory with that measured simultaneously for carbon dioxide.[9–12] They found the ideal P_AG for isoflurane (calculated from adjustment of end-tidal isoflurane partial pressure for alveolar deadspace from equation 1) and $Pc'G$ (from arterial isoflurane partial pressures adjusted for venous admixture) were significantly different. They postulated this difference was due to a diffusion gradient for these heavy molecules within the terminal airways, alveoli, and/or alveolar-capillary membrane (longitudinal diffusion limitation) not considered in the Riley model.

However, these authors overlooked that well-described multicompartment models of lung gas exchange, using physiologically realistic distributions of $\dot{V}_A/\dot{Q}$ scatter, predicted that A-a gradients and alveolar deadspace are different for gases with different blood solubilities, regardless of other factors.[13–15] Nevertheless, it is possible that both blood solubility and diffusion limitation contribute to the observed A-a gradients for volatile agents. Using such multicompartment models of $\dot{V}_A/\dot{Q}$ scatter may help determine the relative contribution of these two factors, and better predict inhalational anesthetic pharmacokinetics. Such models need to be calibrated and tested against measured data.

We extended the study of Landon *et al.*[9] to compare theoretical ideal PAG and $Pc'G$ for four volatile anesthetic agents. We hypothesized that alveolar deadspace fraction (V_{DA}/V_A) calculated from the A-a carbon dioxide partial pressure gradient is different from that calculated from measurements of volatile agents, due to differences in blood gas solubility.

We further hypothesized that a multicompartment computer model of lung gas exchange with physiologically realistic "log-normal" distributions of $\dot{V}_A/\dot{Q}$ scatter would accurately predict measurements of A-a gradients and V_{DA}/V_A for each volatile agent based on its blood solubility, relative to simultaneous measurements made for carbon dioxide, and would thus help explain the differences between these gases in their lung kinetics.[13–15]

Materials and Methods

Clinical Study

We conducted an observational study combining retrospective data obtained from a previous investigation in patients undergoing inhalational anesthesia for cardiac surgery with prospectively collected data in a similar population, forming two series. In both series, arterial and end-tidal carbon dioxide partial pressures and blood oxygen content were measured simultaneously with the volatile anesthetic partial pressure cascade (the declining gradient in partial pressure between inspired gas and mixed venous blood) for four groups of patients, each administered a different volatile anesthetic agent spanning a range of blood-gas partition coefficients, during near steady-state phase inhalational anesthesia.

In both series, data were obtained from patients undergoing elective cardiac or thoracic aortic surgery, with no history of acute or chronic respiratory disease, who were recruited with written informed patient consent. With institutional review board approval (METC97/114 A/mF, 1997), the first series was conducted at Catharina Hospital, Eindhoven, The Netherlands, and Onze-Lieve-Vrouw (OLV) Hospital, Aalst, Belgium, from 1997 to 2000, and recruited 32 patients who were sequentially allocated to receive maintenance phase inhalational general anesthesia with halothane (n = 11), sevoflurane (n = 11), or isoflurane (n = 10). This study was conducted to measure the time course of alveolar-capillary uptake rate of these volatile agents using the direct Fick method, and results of this study from 28 of these patients were previously published.[16] The second series was conducted at the Austin Hospital, Melbourne, Australia, from 2017 to 2019, after ethics review and approval (HREC/16/Austin/419, October 21, 2016), and recruited 30 patients who received sevoflurane (n = 10), desflurane (n = 10), or isoflurane (n = 10) in similar fashion, with all data collected prospectively for the purposes of the current study.

In both series, anesthesia management consisted of routine patient cardiovascular monitoring with peripheral arterial and pulmonary artery catheters, along with continuous tidal gas concentration monitoring and arterial and mixed venous blood gas analysis on at least one occasion in the precardiopulmonary bypass period. After intravenous induction of anesthesia and tracheal intubation, the patient was connected to a circle breathing system with fresh carbon dioxide absorber to eliminate carbon dioxide rebreathing. Tidal volume was set at 7 to 10 ml/kg with 5 cm H_2O positive end-expiratory pressure, and respiratory rate set so as to achieve an end-tidal carbon dioxide partial pressure (P_{ETCO_2}) of 25 to 35 mmHg, with an inspired to expired ratio that ensured a smooth and flat phase 3 plateau on the capnogram. Maintenance anesthesia consisted of inhalational agent without nitrous oxide. Delivered concentrations of oxygen and volatile agent were set to achieve a fractional inspired oxygen

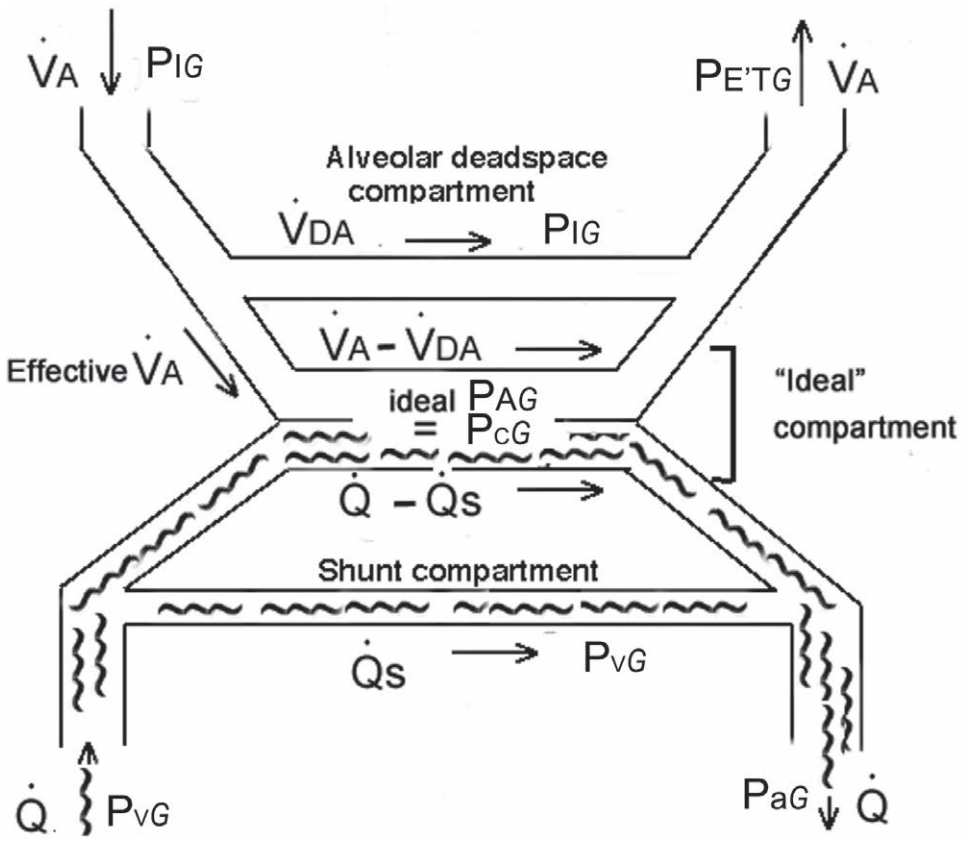

Fig. 1. The three-compartment model of inhomogeneity of ratios of alveolar ventilation ($\dot{V}_A$) to blood flow ($\dot{Q}$) in the lung ($\dot{V}_A/\dot{Q}$ scatter) using a continuous flow principle, where both alveolar deadspace ventilation ($\dot{V}_{DA}$) and shunt blood flow (s) are depicted as shunts, as described by Riley.[8] Partial pressures (inspired [P_{IG}], end-tidal [P_{ETG}], arterial [P_{AG}], mixed venous [P_{vG}], ideal alveolar [ideal P_{AG}] and end-capillary [$P_c'_G$]) of inert gas *G* are also shown.

tension of 50 to 60%, and end-tidal concentrations of 0.5 to 0.75 minimum alveolar concentration (MAC), with or without supplementary intravenous propofol infusion and opioid at the anesthesiologist's discretion to maintain adequate depth of anesthesia determined by clinical assessment and/or processed electroencephalograph monitoring.

During near steady-state maintenance phase inhalational anesthesia, between 30 and 90 min postinduction of anesthesia and before cardiopulmonary bypass, and during a period of stability (less than 10% change over at least a 5-min period of time) in ventilation settings, heart rate, mean arterial blood pressure, and end-expired concentration of carbon dioxide and volatile agent, cardiac output was measured by right heart thermodilution, and simultaneous paired arterial and mixed venous blood samples were collected, along with recording of inspired and end-tidal concentrations of oxygen, carbon dioxide, and volatile agent G (P_{IG} and P_{ETG}) by side-stream gas sampling using a Datex-Ohmeda M-CAiOVX gas analyzer (GE Healthcare, USA; Series 1), or a Datex-Ohmeda Capnomac Ultima gas analyzer (GE Healthcare) connected to a notebook computer (Macbook Air, Apple Corp., USA) running LabVIEW 2011 software (National Instruments, USA), *via* an analog-digital converter card (USB 6009, National Instruments; Series 2).

Blood samples were processed for measurement of respiratory blood gases on a Radiometer ABL 700 (Series 1) or a Radiometer ABL 800 gas analyzer (Series 2) calibrated according to the manufacturer's specifications (Radiometer, Denmark). Volatile agent partial pressures for each gas *G* in arterial (P_{AG}) and mixed venous (P_{vG}) blood were measured by gas analysis after equilibration with 10 ml of headspace gas in gas-tight glass containers. In Series 1 headspace gas analysis was performed using gas chromatography on a Carlo Erba GC 6300 gas chromatograph (Vega Interscience, The Netherlands) with flame ionization detector. In Series 2, headspace gas analysis was performed by the same infrared gas analyzer used to measure tidal gas concentrations, using a method previously described.[17] The linearity of both devices was confirmed by construction of calibration curves using

stock solutions of sevoflurane, isoflurane, and halothane encompassing the clinical range of partial pressures (5 to 80 mcg/l; Series 1), and using eightfold serial 50% dilutions of prepared mixtures of each agent in oxygen/air (Series 2). The infrared rapid gas analyzers used to measure both carbon dioxide and volatile agent had 10 to 90% response times of approximately 360 ms, allowing accurate measurement of end inspired and expired gas partial pressures in tidal gas sampling at the respiratory frequencies used (10 to 14 breaths per min), and of headspace gas sampling for measurement in blood samples.[17] All measured partial pressures were corrected to body temperature, pressure and water vapor saturated. Partial pressures were calculated from those measured after equilibration using the mass balance principle assuming blood/gas partition coefficients for each agent G ($\lambda_{b/g}G$) equal to published values at 37°C, in a population of similar age (halothane = 2.4, isoflurane = 1.45, sevoflurane = 0.74, desflurane = 0.57).[18]

Three-compartment Model Calculated Variables

Calculated variables were obtained using measured input values for $P_{ET}G$, P_AG, $P_{\bar{v}}G$, and inspired (P_IG) partial pressures for each volatile agent *G*, as well as measured partial pressures of carbon dioxide and blood content of oxygen. The methods used followed that used by Landon *et al.*[9] employing the three-compartment model of $\dot{V}_A/\dot{Q}$ scatter, depicted as a continuous flow model in figure 1. The equations used in the calculations are given in the appendix.

A "dilution factor" equivalent to alveolar deadspace fraction for carbon dioxide (V_{DA}/V_{ACO_2}) was calculated from generalization of the Bohr–Enghoff mixing principle, using measured P_{ETCO_2} and P_{ACO_2}. Alveolar deadspace fraction for each volatile agent *G* (V_{DA}/V_AG) was calculated from the measured $P_{ET}G$, P_IG, and P_AG using the same mixing principle as for calculation of V_{DA}/V_{ACO_2}.

Alveolar ventilation rate ($\dot{V}_A$) was calculated from P_{ETCO_2} and the carbon dioxide elimination rate ($\dot{V}_{CO_2}$), estimated from the measured oxygen uptake rate ($\dot{V}_{O_2}$, calculated from the direct Fick principle) assuming a respiratory quotient (RQ) of 0.8 (as $\dot{V}_{CO_2}$ was not directly measured in the study). Effective (*i.e.*, non-deadspace) alveolar ventilation rate (effective $\dot{V}_A$) was then calculated for each agent G and for carbon dioxide from $\dot{V}_A$ and their calculated alveolar deadspace fraction.

The ideal P_AG was calculated from measured $P_{ET}G$ corrected for the contribution of alveolar deadspace to end-tidal gas partial pressure, using the "dilution factor" (V_{DA}/V_{ACO_2}). Pc'*G* was calculated from P_AG corrected for the contribution of calculated venous admixture (Qs/Q) and measured $P_{\bar{v}}G$.

Multicompartment Computer Modeling

Using a previously published multicompartment computer model of $\dot{V}_A/\dot{Q}$ scatter,[19,20] predicted values for each volatile agent *G* of $P_{ET}G$, P_AG and gas uptake rate ($\dot{V}G$) were calculated from flow weighted means of outputs of 50 parallel lung compartments modeling continuous flow in each lung compartment *n* of pulmonary blood flow ($\dot{Q}n$) and expired alveolar ventilation ($\dot{V}_An$). Generic log normal distributions of $\dot{Q}n$ and $\dot{V}_An$ were generated, with the ability to control the degree of $\dot{V}_A/\dot{Q}$ scatter across the 50 lung compartments quantified by the log SD of the distributions according to the method described by West.[13] Steady-state gas exchange in each lung compartment was computed from mass balance according to the Fick principle simultaneously for every alveolar gas using an iterative method, as described by Olszowska and Wagner,[15] as given in the appendix, incorporating the dissociation curve for oxygen and carbon dioxide according to the equations of Kelman.[21,22]

Input values to the model for P_IG, P_{IO_2}, P_{IN_2}, $P_{\bar{v}}G$, and for summated $\dot{V}_{O_2}$, $\dot{Q}$, and $\dot{V}_A$ across all compartments matched the mean measured values listed in table 1 for these variables, and matched mean $\dot{Q}$ and $\dot{V}_A$ measured in each volatile agent group. Input $\dot{V}_{CO_2}$ assumed an overall RQ of 0.8. $\lambda_{b/g}G$ for each volatile agent *G* were as listed above and $\lambda_{b/g}N_2$ was 0.014, and total nitrogen flux in the lung was assumed to be zero. Using a further iterative step, the simulated logSD of $\dot{Q}$ and $\dot{V}_A$ was found so as to generate values for both P_{ETCO_2} and P_{ACO_2} (and therefore V_{DA}/V_{ACO_2}) that matched the mean of values measured in each volatile agent group. Using this logSD, the final output values for $P_{ET}G$ and P_AG were obtained, and V_{DA}/V_AG for each volatile agent predicted from the multicompartment model was then obtained using equation A6 (see appendix).

Statistical Analysis

The *a priori* primary endpoint was the relationship between measured V_{DA}/V_AG for each volatile agent *G* (equation A6) and its log blood/gas partition coefficient ($\lambda_{b/g}G$), determined by linear regression analysis.

Preplanned secondary endpoints were as follows:

(a) Difference ($dV_{DA}/V_AG\text{-}CO_2$) between simultaneous measurements in individual patients of V_{DA}/V_{ACO_2} and V_{DA}/V_AG (equation 1 and equation A6) using Bland–Altman analysis and Pitman's test of difference in variance, and its relationship to $\lambda_{b/g}G$, using linear regression analysis
(b) Difference between calculated V_{DA}/V_AG and that predicted by multicompartment computer modeling
(c) Difference between calculated ideal P_AG (equation A2) and Pc'*G* (equation A5) to assess the validity of the three-compartment model applied to each volatile agent

Comparison of mean values with the *t* test was used where distributions of data were consistent with a normal distribution according to the Shapiro–Wilk test, reporting SD or 95% CI. Otherwise, median values and interquartile range

and nonparametric statistical tests (Kruskal–Wallis equality-of-populations rank test) were used. All statistical comparisons were two-tailed, with a threshold of significance of $P < 0.05$, and analysis was done using Stata 12 (StataCorp, USA). No *a priori* statistical power calculation was made, and the sample size in Series 2 was based on estimation of expected a-a partial pressure differences observed in previous published studies, and predicted values generated by generic multicompartment modeling of typical input data.[9–11,20] All complete sets of data available from patients in Series 1 were included, and clinical data from the two series were collated and analyzed for the purposes of the current study after completion of Series 2.

Results

In Series 1, mixed venous blood gas samples or cardiac output measurements at the required point in time in the pre-cardiopulmonary bypass period were not available for 10 patients, and these were therefore excluded from the pre-planned analysis. A complete set of retrospective data was therefore available from 22 patients (sevoflurane [n = 6], isoflurane [n = 7], and halothane [n = 9]) in Series 1, and prospective data from all 30 patients in Series 2 (sevoflurane [n = 10], isoflurane [n = 10], and desflurane [n = 10]), totaling 52 patients.

Demographic Data

The mean ± SD age of included patients was 66 ± 11 yr, and body mass index was 29 ± 6 kg/m^2. V_{DA}/V_{ACO_2} was similar overall between patients in the two series (mean difference [CI], –0.02 [–0.06 to 0.01], $P = 0.212$ on the unpaired t test) as was $d V_{DA}/V_{AG}\text{-}CO_2$ (mean difference [CI], 0.01 [–0.05 to 0.07], $P = 0.629$ on the unpaired t test). Data from the two series were therefore combined, resulting in four groups of patients each administered one of the four volatile anesthetic agents. Mean MAC achieved at time of sampling was 0.69 for halothane, 0.56 for isoflurane, 0.54 for sevoflurane, and 0.57 for desflurane. Median (interquartile range) time of sample collection was 55 (45, 60) min after induction of anesthesia overall and was similar in the four volatile agent groups ($P = 0.561$ on linear regression analysis).

Physiologic Variables and Partial Pressures

Measured mean ± SD values for $\dot{Q}$, hemoglobin concentration, P_{ACO_2}, and P_{ETCO_2} are shown in table 1. Calculated values for $\dot{V}CO_2$ and $\dot{V}A$, and Qs/Q in each group are also shown, along with the alveolar-capillary uptake rate of the agent in each group ($\dot{V}G$) calculated from measured rate $\dot{Q}$, P_{AG}, $P\bar{v}G$, and $\lambda_{b/g}G$ for each agent using the direct Fick method. Table 2 shows the measured partial pressure cascade (P_{IG}, P_{ETG}, P_{AG}, and P_{VG}) for all four volatile agents.

Three-compartment Model Calculations

Alveolar deadspace fractions for volatile agent used (V_{DA}/V_{AG}) and for carbon dioxide (V_{DA}/V_{ACO_2}) in each of the four groups are given in table 3 and plotted in figure 2 in relation to blood gas partition coefficient for each agent ($\lambda_{b/g}G$). First order best fit curves obtained from least squares analysis for both V_{DA}/V_{AG} and V_{DA}/V_{ACO_2} are plotted (*solid lines*).

Alveolar deadspace fraction for volatile agent was strongly inversely related to blood solubility (V_{DA}/V_{AG} *vs.* $\lambda_{b/g}G$ slope [CI], –0.10 [–0.13 to –0.06], $P < 0.001$ on linear regression analysis; fig. 2). V_{DA}/V_{ACO_2} was weakly inversely related to $\lambda_{b/g}G$ (slope [CI], –0.04 [–0.07 to –0.01], $P = 0.014$ on linear regression analysis; fig. 2). Mean ± SD of V_{DA}/V_{ACO_2} overall was 0.23 ± 0.07. Alveolar deadspace was significantly larger for each volatile agent than for carbon dioxide. Mean difference (CI) between V_{DA}/V_{ACO_2} and V_{DA}/V_{AG} overall was –0.34 (–0.37 to –0.31), Pitman's test of difference in variance was r = –0.42, and $P = 0.009$.

The difference between alveolar deadspace for each volatile agent and carbon dioxide ($dV_{DA}/V_{AG}\text{-}CO_2$) is shown as a function of $\lambda_{b/g}G$ in figure 3 with the best fit curve, and in table 3. There was a significant inverse relationship (slope [CI], –0.06 [–0.10 to –0.02], $P = 0.008$ on linear regression analysis), which reflects that in figure 2, but controls for differences between individuals in $\dot{V}A/\dot{Q}$ scatter measured using V_{DA}/V_{ACO_2}.

The effective alveolar ventilation rate for each volatile agent increased with blood solubility. Calculated from equation A9, mean effective $\dot{V}A$ was 1.0 l/min for desflurane, 1.4 l/min for sevoflurane, 1.4 l/min for isoflurane, and 1.6 l/min for halothane. Effective $\dot{V}A$ for carbon dioxide in each group (from equation A8) was considerably larger, ranging between 2.1 and 2.6 l/min (table 3).

The measured partial pressure cascade for each volatile agent is shown in figure 4 and table 2. Ideal P_{AG} and Pc'_G for each agent calculated from equations A2 and A5 are included. A significant difference between ideal P_{AG} and Pc'_G was found overall and for each of the agents except desflurane (halothane, $P < 0.001$, isoflurane, $P < 0.001$, sevoflurane, $P = 0.004$, desflurane, $P = 0.396$; table 2; for all four agents combined, median [interquartile range], P_{AG} 5.1 [3.7, 8.9] *vs.* Pc'_G 4.0 [2.5, 6.2], $P = 0.011$ on the Kruskal–Wallis test). There was no significant difference in calculated venous admixture (Qs/Q) between groups (table 1).

Multicompartment Model Predictions

The values for input variables in each group for the multicompartment model ($\dot{V}A$ and measured $\dot{Q}$, $\dot{V}CO_2$, Hb, P_{ETCO_2}, P_{ACO_2}, P_{IG}, and P_{VG}) are listed in tables 1 and 2, and those for output variables (predicted P_{ETG}, P_{AG}, V_{DA}/V_{AG}, and $dV_{DA}/V_{AG}\text{-}CO_2$) are shown in table 4.

Theoretical distributions generated by the model of alveolar-capillary uptake rates for the volatile agent in each

Table 1. Measured Values (mean ± SD) for Each Patient Group of Pulmonary Blood Flow Rate ($\dot{Q}$), Hemoglobin Concentration (Hb), Fractional Inspired Oxygen Tension (F_{IO_2}), and Measured Arterial ($Paco_2$) and End-tidal (P_{ETCO_2}) Partial Pressures

Group(n)	$\dot{Q}$ l/min	Hb g/dl	F_{IO_2} %	P_{ETCO_2} mmHg	$Paco_2$ mmHg	$\dot{V}co_2$ l/min	$\dot{V}_A$ l/min	$\dot{V}_G$ ml/min	Qs/Q %
Halothane (n = 9)	4.5 ± 1.1	11.5 ± 1.7	62 ± 12	30 ± 4.2	38.3 ± 6.7	*0.13 ± 0.02*	*3.0 ± 0.6*	*6.6 ± 4.2*	*11.7 ± 4.8*
Isoflurane (n = 17)	4.4 ± 1.1	12.2 ± 1.5	56 ± 7	31 ± 5.4	38.4 ± 6.7	*0.14 ± 0.04*	*3.2 ± 0.7*	*8.0 ± 4.1*	*13.8 ± 6.4*
Sevoflurane (n = 16)	4.6 ± 1.2	12.1 ± 2.2	62 ± 14	29 ± 2.4	39.2 ± 3.9	*0.14 ± 0.06*	*3.6 ± 1.3*	*7.9 ± 3.9*	*12.0 ± 7.6*
Desflurane (n = 10)	4.1 ± 1.2	13.1 ± 1.3	56 ± 11	31 ± 3.7	42.0 ± 4.1	*0.13 ± 0.04*	*2.9 ± 0.8*	*15.3 ± 8.9*	*14.2 ± 5.5*

Calculated carbon dioxide elimination rate ($\dot{V}co_2$), alveolar ventilation rate ($\dot{V}_A$), alveolar-capillary uptake rate ($\dot{V}_G$), and venous admixture (Qs/Q) in each group are also shown in italics.

Table 2. Partial Pressure Cascade for the Four Volatile Agents *G*: Inspired (PI*G*), End-tidal (PET*G*), Arterial (Pa*G*), Mixed Venous (Pv*G*), Ideal Alveolar (ideal PA*G*), and End-pulmonary Capillary (Pc*G*) Partial Pressures in Each Group and Overall

	Partial Pressure mmHg Mean ± SD or Median (Interquartile Range)					
	Measured		*Calculated*		Measured	
Group	PI*G*	PET*G*	*Ideal PAG*	*PcG*	Pa*G*	Pv*G*
Halothane (n = 9)	6.0 ± 0.8	3.7 ± 0.3	*3.0 ± 0.2**	*1.8 ± 0.3**	1.8 ± 0.3	1.3 ± 0.3
Isoflurane (n = 17)	6.1 ± 1.5	4.6 ± 1.2	*4.2 ± 1.2**	*2.8 ± 0.9**	2.7 ± 0.8	1.8 ± 0.7
Sevoflurane (n = 16)	9.2 ± 2.4	7.7 ± 2.0	*7.2 ± 1.9**	*5.4 ± 1.2**	5.2 ± 1.3	3.6 ± 1.0
Desflurane (n = 10)	27.7 ± 14.1	24.4 ± 12.2	*23.4 ± 11.7*	*19.2 ± 9.7*	18.3 ± 9.3	13.1 ± 6.6
Overall (n = 52)	7.1 (6.1, 11.1)	5.5 (4.0, 9.4)	*5.1 (3.7, 8.9)*†	*4.0 (2.5, 6.2)*†	3.5 (2.3, 6.1)	2.3 (1.5, 4.3)

Measured variables (mean ± SD or median [interquartile range]) are in plain print and calculated variables (from equations A2 and A5) in italics. For each volatile agent, statistically significant differences between ideal PA*G* and Pc*G* are indicated with a symbol (**P* < 0.01, or †*P* = 0.011).

group are shown in figure 5, with displayed values scaled for convenience. For each agent, the area under the curve across the 50 lung compartments is the predicted mean gas alveolar-capillary uptake rate of the agent in each group ($\dot{V}_G$), which is also listed in table 4. Distributions for carbon dioxide and oxygen exchange and pulmonary blood flow and expired alveolar ventilation are also plotted using as inputs the overall (n = 52) mean values for $\dot{V}o_2$, $\dot{V}co_2$, $\dot{V}_A$, and $\dot{Q}$ measured in the study. The log SD of the distribution of $\dot{Q}$ and $\dot{V}_A$ plotted is 1.5, which was the mean of values across the four groups.

As the blood solubility of the agent declined, the predicted distribution of gas uptake shifted further leftward relative to the distribution of carbon dioxide elimination, toward lower $\dot{V}_A/\dot{Q}$ ratio lung compartments, reducing effective alveolar ventilation rate for the agent and therefore increasing alveolar deadspace ventilation. A lower effective $\dot{V}_A$ for volatile agents is explained by the greater reliance of less soluble gases on perfusion-driven uptake in lower $\dot{V}_A/\dot{Q}$ lung compartments, with greater "wasted ventilation" in higher $\dot{V}_A/\dot{Q}$ lung compartments than is the case for carbon dioxide, which more closely follows the distribution of alveolar ventilation.

The predicted values from the multicompartment model of alveolar deadpace fraction V_{DA}/V_{AG} and dV_{DA}/V_{AG}-co_2 for each agent are shown in figures 2 and 3, respectively, with a best fit curve (*broken line*). The slope of the best fit line closely paralleled that of V_{DA}/V_{AG} based on equation A6 found in our patients (*solid line*). However, predicted V_{DA}/V_{AG} underestimated it for all four agents by a similar amount. The predicted (broken) best fit line lay below the 95% CI (*dotted line*) for the observed (*solid*) best fit line (generated using the "lfitci" function in Stata 12) at all points. Consistent with this, predicted $\dot{V}_G$ (table 4) from the model was greater than mean $\dot{V}_G$ measured in each group (table 1). This indicated a contribution to measured alveolar deadspace and inefficiency of gas exchange of anesthetic agents other than that predicted by the effect of solubility alone from equation A10 (appendix).

Discussion

We found that alveolar deadspace for inhaled anesthetic agents, calculated from the three-compartment model of $\dot{V}_A/\dot{Q}$ scatter, is much larger than that calculated simultaneously for carbon dioxide, and its magnitude is linearly

Table 3. Calculated Alveolar Deadspace Fraction for Carbon Dioxide (V_{DA}/V_{ACO_2}) and Volatile Agent *G* (V_{DA}/V_{AG}) in Each Group Based on the Three-compartment Model, and Difference between These dV_{DA}/V_{AG}-CO_2; and Calculated Mean Effective Alveolar Ventilation Rate for Each Volatile Agent (Effective $\dot{V}_A$ for *G*) and for Carbon Dioxide (Effective $\dot{V}_A$ for CO_2)

	Three-compartment Model: Measured Mean ± SD				
Group	**V_{DA}/V_{ACO_2}**	**V_{DA}/V_{AG}**	***d*V_{DA}/V_{AG}-CO_2**	**Effective $\dot{V}_A$ for CO_2**	**Effective $\dot{V}_A$ for *G***
Halothane (n = 9)	*0.21 ± 0.06*	*0.47 ± 0.08*	*0.25 ± 0.10*	*2.4 ± 0.6 l/min*	*1.6 ± 0.4 l/min*
Isoflurane (n = 17)	*0.20 ± 0.06*	*0.55 ± 0.09*	*0.35 ± 0.10*	*2.6 ± 0.6 l/min*	*1.4 ± 0.4 l/min*
Sevoflurane (n = 16)	*0.26 ± 0.06*	*0.61 ± 0.10*	*0.35 ± 0.10*	*2.6 ± 1.0 l/min*	*1.4 ± 0.5 l/min*
Desflurane (n = 10)	*0.26 ± 0.06*	*0.65 ± 0.07*	*0.39 ± 0.10*	*2.1 ± 0.7 l/min*	*1.0 ± 0.3 l/min*

Measured variables (plain type) are distinguished from calculated variables (italics).

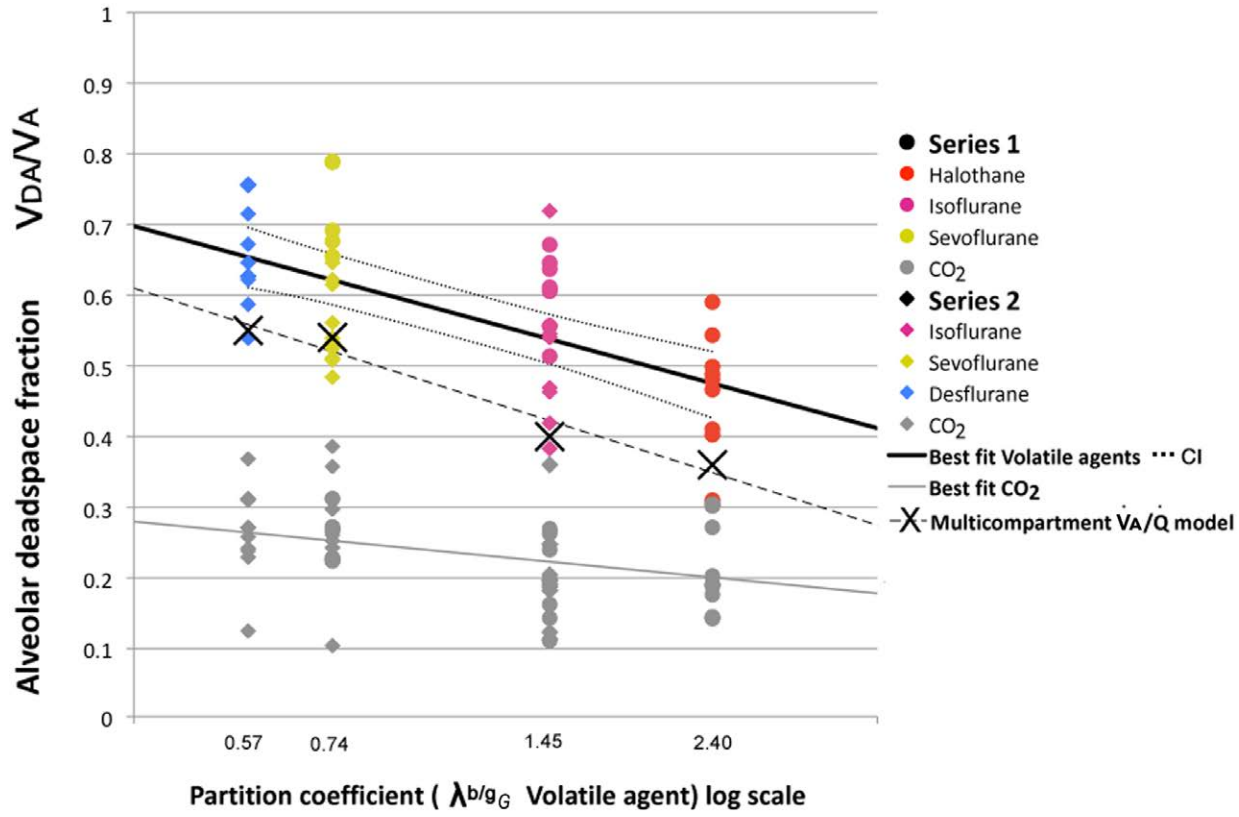

Fig. 2. Alveolar deadspace fraction for carbon dioxide (V_{DA}/V_{ACO_2}) and volatile agents (V_{DA}/V_{AG}) in relation to blood/gas partition coefficient of the agent *G* administered in each of the four groups ($\lambda_{b/g}G$). In Series 1 and 2, measurements of isoflurane, sevoflurane and carbon dioxide were made; in Series 1, halothane was also measured, whereas in Series 2, desflurane was included instead. Linear best fit curves for both V_{DA}/V_{AG} and V_{DA}/V_{ACO_2} are plotted (*solid lines*) with CI (*dotted lines*). Crosses with linear best fit curve (*broken line*) indicate the predicted mean value for each group from multi-compartment modeling of a log normal distribution of and $\dot{V}_A$ with a log SD that generated a V_{DA}/V_{ACO_2} equal to the mean measured in the that group.

related to the blood/gas partition coefficient of the agent, increasing substantially as blood solubility declines, while reducing their effective alveolar ventilation rate.

Our data show that the custom of calculating alveolar deadspace using measured A-a partial pressure gradients for carbon dioxide (equation 1) is misleading in predicting the A-a gradients, alveolar deadspace, and effective ventilation rate of other gases with different blood solubilities, such as inhaled agents used in anesthesia, and unhelpful in understanding anesthetic gas exchange. Indeed, our data show

how there is no "definitive" pulmonary alveolar deadspace. In fact, alveolar deadspace fraction for modern anesthetic gases is much greater, and their effective $\dot{V}_A$ is considerably lower than for carbon dioxide, which is more soluble in blood (table 3). Our data show how we must conceive of a range of different ideal and alveolar deadspace compartments simultaneously for gases of different solubilities in the same patient.

These concepts and their clinical implications are poorly understood in the field of anesthesiology and reflect the limitations of the concept of alveolar deadspace as it is customarily measured in helping us understand the kinetics of inhalational agents in the lung. However, the relationship of A-a gradients and alveolar deadspace to blood solubility is predicted by a multicompartment model of $\dot{V}_A/\dot{Q}$ scatter using physiologically realistic log normal distributions of $\dot{V}_A$ and $\dot{Q}$ of the kind shown in figure 5. Despite such physiologic models of gas exchange being first described many years ago by researchers in respiratory physiology,[13–15] commentators in anesthesiology have rarely engaged them in trying to measure or explain observed gas exchange during inhalational anesthesia.

A good example was a long-running misunderstanding of the mechanism and magnitude of the "second gas effect," where the rapid alveolar-capillary uptake of nitrous oxide powerfully concentrates the alveolar and arterial partial pressures of the accompanying volatile agent.[23] This concentrating effect is greatest where the effective $\dot{V}_A$ is low relative to perfusion, as it is for volatile agents as we have shown, as well as for nitrous oxide, but failure to understand this led some commentators to dismiss the second gas effect as insignificant or implausible.[12,24–29]

Our findings have implications for the reliability of measurements of anesthetic gas uptake rates made at the level of the mouthpiece in a breathing circuit. Where end-expired gas partial pressures are measured, an estimate of $\dot{V}_A$ is needed,[30,31] which is traditionally obtained by subtraction from minute ventilation of anatomical deadspace ventilation measured from nitrogen exhalation (Fowler's method).[32] However, our data show how this measurement of $\dot{V}_A$ will not account for the differences in *effective* (non-deadspace) $\dot{V}_A$ between gases of different solubilities in blood. Attempts to estimate volatile agent lung uptake rates this way can be widely inconsistent with definitive measurements made invasively from the Fick principle (from measured pulmonary blood flow and arterial and mixed venous partial pressures).[33]

More generally, failure by simple models of lung gas exchange to account for realistic A-a gradients due to $\dot{V}_A/\dot{Q}$ scatter makes them potentially misleading.[16] Such models, while useful teaching tools, can be unreliable tools

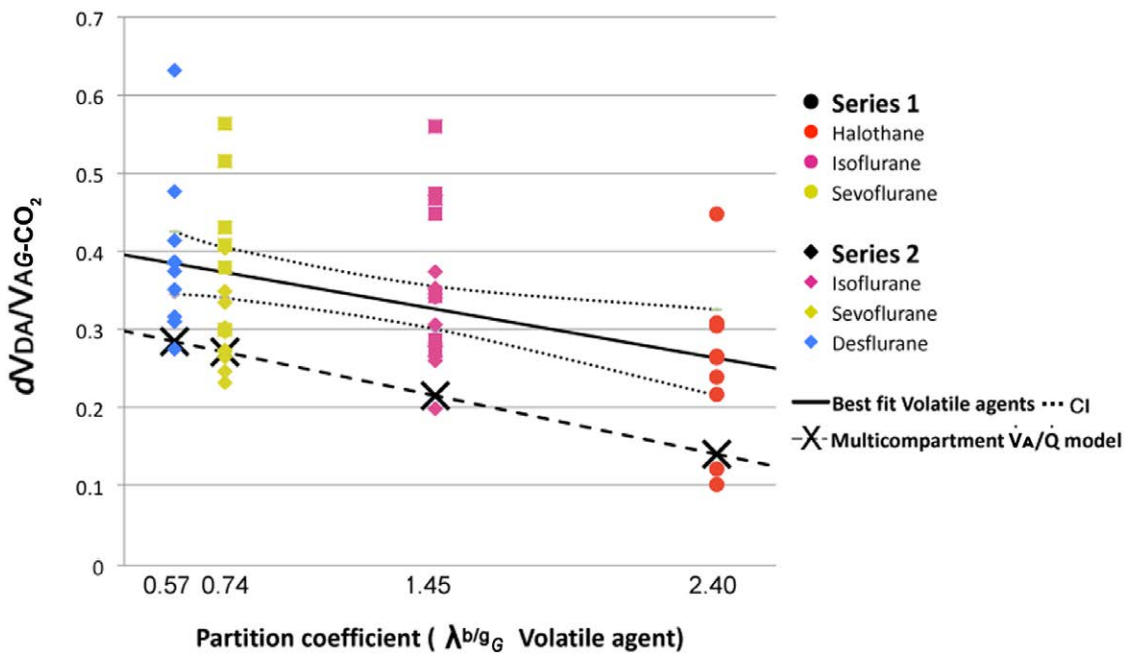

Fig. 3. Difference (dVDA/VAG-CO$_2$) between alveolar deadspace fraction for carbon dioxide (VDA/VACO$_2$) and volatile agents (VDA/VAG) measured in each patient, and linear best fit (*solid line*) with CI (*dotted lines*), in relation to blood/gas partition coefficient of the agent G administered in each of the four groups ($\lambda_{b/g}G$). In Series 1 and 2, measurements of isoflurane, sevoflurane and carbon dioxide were made; in Series 1, halothane was also measured, whereas in Series 2, desflurane was included instead. Crosses with linear best fit curve (*broken line*) indicate the predicted mean value for each group from multicompartment modeling of a log normal distribution of $\dot{Q}$ and $\dot{V}_A$ with a log SD that matched the mean measured VDA/VACO$_2$ in that group.

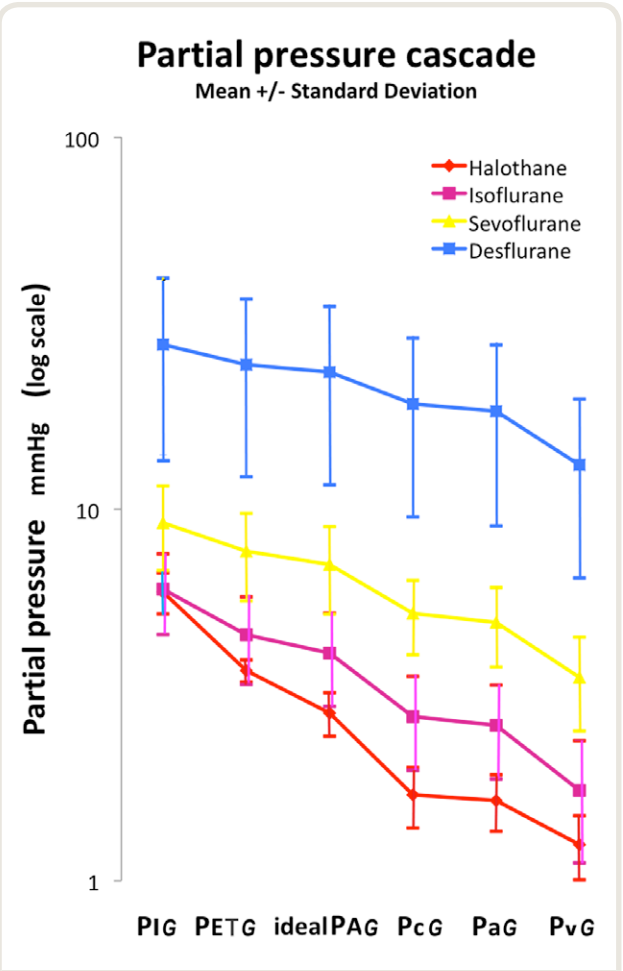

Fig. 4. Partial pressure cascade for all four volatile agents. Mean ± SD (error bars) of measured inspired (P_{IG}), end-tidal (P_{ETG}), arterial (P_{AG}), and mixed venous (P_{vG}) partial pressures for each agent *G* are plotted (table 2). Calculated ideal alveolar (ideal P_{AG}) and end-pulmonary capillary ($P_c'_G$) partial pressures are included for each agent from equations A2 and A5, respectively.

for physiologic modeling and research purposes. This simplistic approach is encouraged by our clinical experience, where reliance on tidal gas concentration monitoring as a routine tool for assessing anesthetic delivery and depth is reinforced by the concept of MAC, which focuses entirely on end-expired gas concentration measurements. Indeed, MAC effectively achieves its clinical purpose while ignoring the existence of an A-a gradient, which is typically 15 to 30% of end-tidal volatile agent partial pressure.[9–12,33] Although clearly vital clinical tools, end-tidal measurements can be insufficient as investigative tools when considering the physiology and pharmacokinetics of inhalational anesthesia. In contrast, the concept of substantial A-a gradients, which are different for different gases, has been familiar to respiratory physiologists for many years, in particular to advocates of the Multiple Inert Gas Elimination Technique, which uses expired to arterial partial pressure gradients measured for several gases across a wide range of blood solubilities to recover, in reverse fashion, $\dot{V}_A/\dot{Q}$ distributions in the lung.[34,35]

Our data show a substantial difference between ideal P_{AG} and $P_c'_G$ calculated from alveolar deadspace based on carbon dioxide measurements, and the shunt equation based on oxygen content measurements. This was true for the agents we studied overall, and individually except desflurane (where greater variability in inspired partial pressure in this patient subgroup at the time of sampling produced excessive scatter in other measured partial pressures). This difference between ideal P_{AG} and $P_c'_G$ was first demonstrated by Landon *et al.* for isoflurane.[9] These authors suggested diffusion limitation of these heavy molecules within the terminal airways, or at the alveolar-capillary barrier, not considered by three-compartment theory, to explain this. They did not discuss that published multicompartment models using physiologic distributions of $\dot{V}_A/\dot{Q}$ scatter predicted that gas solubility in blood strongly determines A-a gradients, and would explain much of their findings.[13–15] Our data from a multicompartment model confirm this, and furthermore accurately predict the difference between agents (slope) in V_{DA}/V_{AG} based on differences in blood solubility (figs. 2 and 3).

However, while the slope of the relationship of V_{DA}/V_{AG} to blood-gas partition coefficient was predicted, the magnitude of the difference in V_{DA}/V_A between each agent and carbon dioxide was underestimated by the multicompartment model (figs. 2 and 3). As equation A10 (appendix) indicates, blood solubility was the only characteristic of the inert gas computed by multicompartment models such as ours. The residual difference between calculated $d(V_{DA}/V_{AG}\text{-}CO_2)$ and that predicted by the model implies a contribution to the V_{DA}/V_{AG} observed in our patients other than solubility alone. A diffusion-limited basis for this residual difference in alveolar deadspace fraction, involving limitation to longitudinal gas mixing in terminal airways, and possibly to alveolar-capillary gas transfer, remains highly plausible given the high molecular weight of these agents compared to carbon dioxide.[36,37] The fact that this residual difference we have demonstrated (approximately 10% of V_{DA}/V_{AG}) was similar in magnitude for all four agents supports diffusion-limitation as a mechanism, given that they have comparable molecular weights (between 168 and 200) and would be expected to exhibit roughly similar diffusion characteristics in the terminal airways and alveolus. Further research to distinguish the contributions of blood solubility and diffusion-limitation to A-a partial pressure gradients and inefficiency of gas exchange of inhalational anesthetic agents is indicated.

We found a weak relationship between V_{DA}/V_{ACO_2} and volatile agent group in our study, which was an unexpected but interesting finding, given that the agents were administered at similar proportions of MAC but different inspired concentrations. The suggestion that the agents might exert a differential effect on overall $\dot{V}_A/\dot{Q}$ matching in the

Table 4. Output Results from the Multicompartment Model of Physiologically Realistic, Log-normal Distributions of VA/Q Ratios

	Output Values (for Modeling Inputs See Tables 1 and 2)					
Group	**log SD**	**PET*G* mmHg**	**Pa*G* mmHg**	**V_{DA}/V_{AG}**	***d*V_{DA}/V_{AG}-CO_2**	**$\dot{V}_G$ *ml/min***
Halothane	*1.47*	*3.47*	*1.99*	*0.36*	*0.15*	*11.3*
Isoflurane	*1.37*	*4.06*	*2.80*	*0.40*	*0.20*	*9.3*
Sevoflurane	*1.55*	*7.45*	*5.48*	*0.54*	*0.28*	*9.4*
Desflurane	*1.56*	*23.6*	*18.8*	*0.55*	*0.29*	*18.4*

Input values to the model for each patient group were mean measured arterial ($Paco_2$) and end-expired ($Petco_2$) partial pressures, pulmonary blood flow rate ($\dot{Q}$), carbon dioxide elimination rate ($\dot{V}co_2$), alveolar ventilation rate ($\dot{V}_A$), hemoglobin concentration (Hb), and inspired (PI*G*), and mixed venous (Pv*G*) partial pressures of volatile agent *G* administered, and are given in tables 1 and 2. Output values from the model are listed for predicted mean end-tidal partial pressure PET*G* and arterial partial pressure Pa*G*, and predicted alveolar deadspace fraction (V_{DA}/V_{AG}) for the volatile anesthetic agent *G* administered, and the difference between this and V_{DA}/V_{ACO_2} (*d*V_{DA}/V_{AG}-CO_2), and predicted alveolar-capillary uptake rate ($\dot{V}_G$) in each patient group. The log SD of the distribution of VA/Q that generated the measured input $Petco_2$, $Paco_2$ and V_{DA}/V_{ACO_2} in each group is listed. Measured variables (plain type) are distinguished from calculated variables (italics).

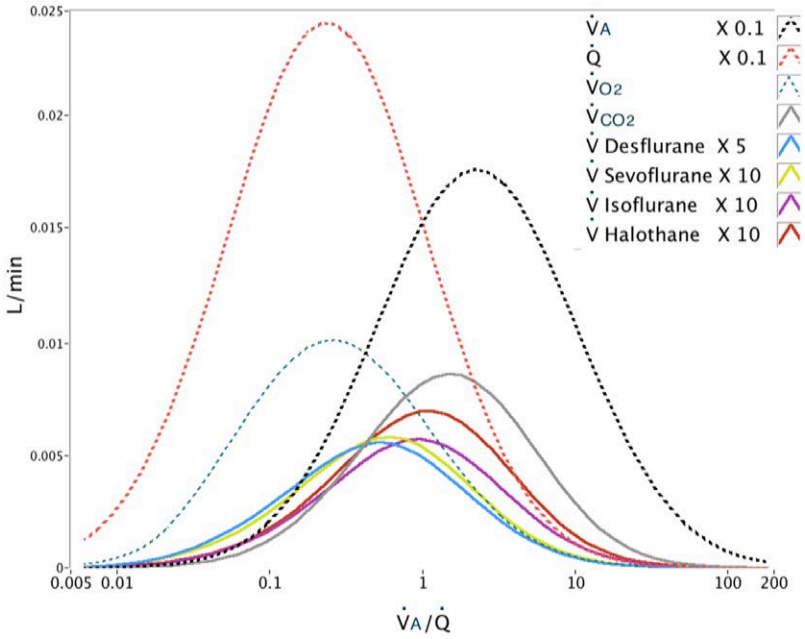

Fig. 5. Composite diagram of distributions of predicted rates of alveolar-capillary gas uptake ($\dot{V}_G$) for each volatile agent ($\dot{V}$ Desflurane, $\dot{V}$ Sevoflurane, $\dot{V}$ Isoflurane and Halothane) generated by a 50 compartment model of inhomogeneity with log normal distributions of alveolar ventilation ($\dot{V}_A$) and pulmonary blood flow, and of oxygen uptake ($\dot{V}o_2$) and carbon dioxide elimination ($\dot{V}co_2$) rates, using values for mean inspired, end-tidal, arterial, and mixed venous partial pressures for each agent and carbon dioxide and blood oxygen content measured in the study. The log SD of the distribution of $\dot{Q}$ and $\dot{V}_A$ plotted here was 1.5, representing the calculated mean across all four patient groups. Displayed $\dot{V}_A$, $\dot{Q}$, and $\dot{V}_G$ for each volatile agent are scaled as indicated for convenience.

lung related to either blood solubility or alveolar concentration, but not to anesthetic depth, is interesting but is unsupported by the similar mean venous admixture calculated across all four groups, suggesting a similar degree of impairment of hypoxic pulmonary vasoconstriction by the agents.[1]

A limitation of our study is that we used generic log normal $\dot{V}_A/\dot{Q}$ distributions for the purposes of our multicompartment modeling, and did not collect data using, for example, the Multiple Inert Gas Elimination Technique, to measure individualized patient $\dot{V}_A/\dot{Q}$ distributions, which may, for instance, be multimodal in shape. However, this modeling simulated log SD values that predicted identical A-a partial pressure gradients for carbon dioxide to the mean of those measured in each patient group we studied (table 1) and therefore is likely to represent the mean

predicted behavior of each agent relative to carbon dioxide with acceptable precision for each patient group.

The combining of retrospective and prospective data collected from the two series conducted at different times can be seen as both a limitation and a strength of this study. Importantly, it allowed combination of data on halothane and desflurane, with widely different blood solubilities. Although the clinical protocols of the two studies were similar, the equipment and methodologies for measurement of anesthetic agent in blood in the two series were different. However, the similar findings in these two series of V_{DA}/V_{AG} for both isoflurane and sevoflurane relative to V_{DA}/V_{ACO_2} reinforce the reproducibility and validity of our overall findings.

In conclusion, measurement of the partial pressure cascade for inhaled anesthetic agents shows that pulmonary alveolar deadspace fraction for these agents is much larger than that conventionally calculated from arterial to end-tidal carbon dioxide partial pressure gradients, and that this is a function of the different solubility of the agents in blood. This makes estimates of the effect of $\dot{V}_A/\dot{Q}$ scatter on inhalational anesthetic gas kinetics in the lungs, using measurements of $\dot{V}_A/\dot{Q}$ scatter made this way according to the traditional three-compartment model, misleading. Physiologically realistic multicompartment modeling of $\dot{V}_A/\dot{Q}$ scatter describes the relative differences in A-a partial pressure gradients and alveolar deadspace of inhalational agents accurately, but also suggests a residual component of the A-a gradient that could potentially be explained by longitudinal diffusion limitation for these heavy molecules.

Research Support

This work was supported by a project grant from the Australian and New Zealand College of Anaesthetists Research Foundation, Melbourne, Australia, and by an internal research grant of the Catharina Hospital, Eindhoven, The Netherlands, and an internal research grant of the Onze-Lieve-Vrouw (OLV) Hospital, Aalst, Belgium.

Competing Interests

Dr. Peyton has received research consultancy payments from Maquet Critical Care/Getinge (Solna, Sweden). Dr. Hendrickx has received lecture support, travel reimbursements, equipment loans, consulting fees, and meeting organizational support from AbbVie (Chicago, Illinois), Acertys (Aartselaar, Belgium), Air Liquide (Paris, France), Allied Healthcare (St. Louis, Missouri), Armstrong Medical (United Kingdom), Baxter (Lessines, Belgium), Dräger (Lübeck, Germany), GE (Madison, Wisconsin), Getinge (Solna, Sweden), Hospithera (Brussels, Belgium), Lowenstein (Karlsruhe, Germany), Intersurgical (United Kingdom), Maquet (Solna, Sweden), MDMS (Loos, France), MEDEC (Aalst, Belgium), Micropore (Elkton, Maryland), Molecular Products (United Kingdom), Philips (Amsterdam, The Netherlands), Piramal (Mumbai, India), and Quantium Medical (Barcelona, Spain). The other authors declare no competing interests.

Correspondence

Address correspondence to Dr. Peyton: Department of Anaesthesia, Austin Health, Heidelberg 3084, Australia. phil.peyton@austin.org.au. This article may be accessed for personal use at no charge through the Journal Web site, www.anesthesiology.org.

Appendix

Ideal Alveolar Partial Pressure Calculation

The ideal alveolar partial pressure for volatile agent *G* (ideal P_{AG}) was calculated from measured P_{ETG} corrected for the contribution of alveolar deadspace to end-tidal gas partial pressure, using a "dilution factor" equivalent to alveolar deadspace fraction for carbon dioxide (V_{DA}/V_{ACO_2}) from generalization of the mixing principle of the Bohr–Enghoff equation to the alveolar gas compartment (fig. 1). This uses end-tidal (alveolar) carbon dioxide partial pressure (P_{ETCO_2}), and also uses arterial blood (Pa_{CO_2}) carbon dioxide partial pressure as an approximation of ideal Pa_{CO_2}, which ignores the contribution of shunt to Pa_{CO_2}, because the mixed venous-arterial P_{CO_2} difference is small. Accordingly,[9]

$$V_{DA}/V_{ACO_2} = (P_{ETCO_2} - Pa_{CO_2})/(P_{ICO_2} - Pa_{CO_2}) \quad \text{(A1)}$$

Assuming that no rebreathing of carbon dioxide occurs from the breathing system and inspired carbon dioxide partial pressure (P_{ICO_2}) is zero, this becomes

$$\begin{aligned} V_{DA}/V_{ACO_2} &= -(P_{ETCO_2} - Pa_{CO_2})/Pa_{CO_2} \\ &= 1 - P_{ETCO_2}/Pa_{CO_2} \end{aligned} \quad (1)$$

Ideal P_{AG} was then calculated from[9]

$$\text{ideal } P_{AG} = (P_{ETG} - P_{IG} \times V_{DA}/V_{ACO_2})/(1 - V_{DA}/V_{ACO_2}) \quad \text{(A2)}$$

End-capillary Partial Pressure Calculation

End-capillary partial pressure (Pc'_G) was calculated from Pa_G corrected for the contribution of venous admixture ($\dot{Q}s/\dot{Q}$) and P_{vG}.

$\dot{Q}s/\dot{Q}$ was calculated using measurements of oxygen content in blood according to the shunt equation of Berggren

$$\dot{Q}s/\dot{Q} = (Cc'_{O_2} - CaO_2)/(Cc'_{O_2} - CvO_2) \quad \text{(A3)}$$

where CaO_2 and CvO_2 are arterial and mixed venous blood oxygen content measurements calculated from the measured oxygen hemoglobin saturations and oxygen partial

pressures, and end-capillary oxygen content ($Cc'O_2$) was calculated from ideal P_{AO_2} obtained from the ideal alveolar gas equation and an assumed respiratory quotient (RQ) of 0.8,

$$\text{ideal } P_{AO_2} = P_{IO_2} - P_{aCO_2} / RQ \quad \text{(A4)}$$

and where it is assumed that ideal $P_{AO_2} = Pc'O_2$.

$Cc'O_2$ was calculated from $Pc'O_2$ and the oxyhemoglobin dissociation curve using the equations of Kelman.[21]

$Pc'G$ was then calculated from[9]

$$Pc'G = \left(P_{AG} - P_{vG} \times Qs / Q\right) / (1 - Qs / Q) \quad \text{(A5)}$$

The contribution of shunt in measured P_{aCO_2} used in equations 1 and A4 to error in the calculation of ideal P_{AG} and $Pc'G$ using equations A2 and A5 has been shown to have a negligible influence on these calculations for isoflurane, with an estimated relative adjustment to the alveolar "dilution factor" of approximately 2%, and to calculated ideal PAG and PcG for isoflurane of only 0.4% and 0.05%, respectively, where mean shunt fraction is similar in magnitude to our study.[9]

Alveolar Deadspace Fraction for *G*

Alveolar deadspace fraction for each volatile agent G (V_{DA}/V_{AG}) was calculated from the measured PaG using the same mixing principle as equation 1:

$$V_{DA} / V_{AG} = \left(P_{ETG} - P_{aG}\right) / \left(P_{IG} - P_{aG}\right) \quad \text{(A6)}$$

Alveolar Ventilation and Effective Alveolar Ventilation Rates

Alveolar ventilation rate ($\dot{V}_A$) was calculated from P_{ETCO_2} and the carbon dioxide elimination rate ($\dot{V}_{CO_2}$), estimated from the measured O_2 uptake rate ($\dot{V}_{O_2}$, calculated from the direct Fick principle) assuming a respiratory quotient RQ of 0.8) according to

$$\dot{V}_A \times P_{ETCO_2} / P_B = \dot{V}_{CO_2} = \dot{Q} \times \left(Ca_{O_2} - Cv_{O_2}\right) \times RQ \quad \text{(A7)}$$

where PB was barometric pressure at body temperature and pressure saturated.

Effective (*i.e.*, non-deadspace) alveolar ventilation rate (effective $\dot{V}_A$) was then calculated for each agent G and for carbon dioxide from $\dot{V}_A$ and the calculated alveolar deadspace fraction from equations 1 and A6:

$$\text{Effective } \dot{V}_A \text{ for } CO_2 = \dot{V}_A \times (1 - V_{DA} / V_{ACO_2}) \quad \text{(A8)}$$

and

$$\text{Effective } \dot{V}_A \text{ for } G = \dot{V}_A \times (1 - V_{DA} / V_{AG}) \quad \text{(A9)}$$

Multicompartment Computer Modeling

Using generic log normal distributions of pulmonary blood flow ($\dot{Q}\,n$) and expired alveolar ventilation ($\dot{V}_{AE}n$) (where $\dot{V}_A = \Sigma \dot{V}_{AE}n$ and $\dot{Q} = \Sigma \dot{Q}n$), with a given log SD (logSD) generated as described by West,[13] for each gas *g* (oxygen, carbon dioxide, volatile agent G, and balance gas nitrogen N_2) in each lung compartment *n*,

$$\begin{aligned}\dot{V}gn &= \dot{V}_{AI}n \times P_{IG} / P_B - \dot{V}_A n \times P_A gn / P_B \\ &= \dot{Q}n \times (Cc'gn - Cvg)\end{aligned} \quad \text{(A10)}$$

where

$$\dot{V}_{AI}n = \dot{V}_{AE}n + \dot{V}gn + \dot{V}_{O_2}n + \dot{V}_{CO_2}n + \dot{V}_{N_2}n \quad \text{(A11)}$$

assuming in each compartment that $Pc'gn = P_A gn$ for all gases, where inert gas (volatile agent and N_2) content of end-capillary, arterial, and mixed venous blood ($Cc'g$, Cag, and Cvg) is a product of its partial pressure ($Pc'g$, Pag, and Pvg)/PB and $\lambda_{b/g}$ for *g*, according to Henry's law. The relationships in each lung compartment between partial pressures and blood content of oxygen and carbon dioxide in end-capillary, arterial, and mixed venous blood were calculated from the dissociation curve for oxygen and carbon dioxide according to the equations of Kelman,[21,22] incorporating corrections for measured hemoglobin concentration in each group, and correcting for the wide variation in acid-base balance with $P_{aCO_2}n$ and VA/Q ratio across the 50 compartments modeled.[20]

Flow-weighted mean values for mixed alveolar (end-tidal) partial pressure (P_{ETG}) and mixed end-capillary (arterial) gas content (Cag) were calculated from outputs from all lung compartments:

$$P_{ETG} = \Sigma(P_A gn \times \dot{V}_{AE}n) / \Sigma \dot{V}_{AE}n \quad \text{(A12)}$$

and

$$Cag = \Sigma(Cc'gn \times \dot{Q}n) / \Sigma \dot{Q}n \quad \text{(A13)}$$

and gas uptake rate for each gas *g* was

$$\dot{V}g = \Sigma \dot{V}gn \quad \text{(A14)}$$

References

1. Lumb A: Anaesthesia, Nunn's Applied Respiratory Physiology, 5th edition. Oxford, Butterworth-Heinemann, 2000, pp 440–9
2. Lundh R, Hedenstierna G: Ventilation-perfusion relationships during anaesthesia and abdominal surgery. Acta Anaesthesiol Scand 1983; 27:167–73
3. Lundh R, Hedenstierna G: Ventilation-perfusion relationships during halothane anaesthesia and mechanical ventilation. Effects of varying inspired oxygen concentration. Acta Anaesthesiol Scand 1984; 28:191–8
4. Hedenstierna G, Lundh R, Johansson H: Alveolar stability during anaesthesia for reconstructive vascular surgery in the leg. Acta Anaesthesiol Scand 1983; 27:26–34

5. Dueck R, Young I, Clausen J, Wagner PD: Altered distribution of pulmonary ventilation and blood flow following induction of inhalation anesthesia. Anesthesiology 1980; 52:113–25
6. Bindislev L, Hedenstierna G, Santesson J, Gottlieb I, Carvallhas A: Ventilation-perfusion distribution during inhalation anaesthesia. Acta Anaesth Scand 1981; 25:360–71
7. Rehder K, Knopp TJ, Sessler AD, Didier EP: Ventilation-perfusion relationship in young healthy awake and anesthetized-paralyzed man. J Appl Physiol Respir Environ Exerc Physiol 1979; 47:745–53
8. Riley RL: Development of the three-compartment model for dealing with uneven distribution, Pulmonary Gas Exchange, Volume 1. Ventilation Blood Flow and Diffusion. Edited by West JB. New York, Academic Press Publishers, 1980, pp 67–85
9. Landon MJ, Matson AM, Royston BD, Hewlett AM, White DC, Nunn JF: Components of the inspiratory-arterial isoflurane partial pressure difference. Br J Anaesth 1993; 70:605–11
10. Frei FJ, Zbinden AM, Thomson DA, Rieder HU: Is the end-tidal partial pressure of isoflurane a good predictor of its arterial partial pressure? Br J Anaesth 1991; 66:331–9
11. Dwyer RC, Fee JP, Howard PJ, Clarke RS: Arterial washin of halothane and isoflurane in young and elderly adult patients. Br J Anaesth 1991; 66:572–9
12. Peyton PJ, Horriat M, Robinson GJ, Pierce R, Thompson BR: Magnitude of the second gas effect on arterial sevoflurane partial pressure. Anesthesiology 2008; 108:381–7
13. West JB: Ventilation-perfusion inequality and overall gas exchange in computer models of the lung. Respir Physiol 1969; 7:88–110
14. Farhi LE, Olszowka AJ: Analysis of alveolar gas exchange in the presence of soluble inert gases. Respir Physiol 1968; 5:53–67
15. Olszowska AJ, Wagner PD: Numerical analysis of gas exchange, Pulmonary Gas Exchange. Edited by West JB. New York, Academic Press Publishers, 1980, pp 263, 275–6
16. Hendrickx JFA: The Pharmacokinetics of Inhaled Anaesthetics and Carrier Gases. PhD Thesis, Ghent University Faculty of Medicine and Health Sciences, Department of Anesthesiology, Ghent, Belgium, 2004, pp 73–83, 101–11
17. Peyton P, Chong M, Stuart-Andrews C, Robinson G, Pierce R, Thompson B. Measurement of anesthetic agents in blood using a conventional infrared clinical gas analyzer. Anesth Analg 2007; 105:680–7
18. Esper T, Wehner M, Meinecke CD, Rueffert H: Blood/gas partition coefficients for isoflurane, sevoflurane, and desflurane in a clinically relevant patient population. Anesth Analg 2015; 120:45–50
19. Peyton PJ, Robinson GJ, Thompson B: Ventilation-perfusion inhomogeneity increases gas uptake in anesthesia: Computer modeling of gas exchange. J Appl Physiol (1985) 2001; 91:10–6
20. Peyton P, Robinson G, Thompson B. The effect of ventilation-perfusion inhomogeneity and nitrous oxide on oxygenation in anesthesia: Physiological modeling of gas exchange. J Appl Physiol 2001; 91:17–25
21. Kelman GR: Digital computer subroutine for the conversion of oxygen tension into saturation. J Appl Physiol 1966; 21:1375–6
22. Kelman GR: Digital computer procedure for the conversion of PCO2 into blood CO2 content. Respir Physiol 1967; 3:111–5
23. Stoelting RK, Eger EI II: An additional explanation for the second gas effect: A concentrating effect. Anesthesiology 1969; 30:273–7
24. Lin CY: Uptake of anaesthetic gases and vapours. Anaesth Intensive Care 1994; 22:363–73
25. Lin CY, Wang JS: Supramaximal second gas effect–A nonexistent phenomenon. Anesth Analg 1993; 77:870–2
26. Peyton P: Physiological Determinants during Anaesthesia of the Accuracy of Pulmonary Blood Flow Measurement from Soluble Gas Exchange: Computer Modeling and Patient Measurement. Doctorate of Medicine Thesis, University of Melbourne, Melbourne, Australia, 2004
27. Peyton PJ, Stuart-Andrews C, Deo K, Strahan F, Robinson GJ, Thompson BR, Pierce R: Persisting concentrating and second gas effects on oxygenation during N2O anaesthesia. Anaesthesia 2006; 61:322–9
28. Peyton PJ, Fortuin M, Robinson GJ, Stuart-Andrews C, Pierce R, Thompson BR: The rate of alveolar-capillary uptake of sevoflurane and nitrous oxide following anaesthetic induction. Anaesthesia 2008; 63:358–63
29. Peyton PJ, Chao I, Weinberg L, Robinson GJ, Thompson BR: Nitrous oxide diffusion and the second gas effect on emergence from anesthesia. Anesthesiology 2011; 114:596–602
30. Culver BH: Gas exchange in the lung, Clinical Respiratory Medicine, 3rd edition. Edited by Albert RK, Spiro SG. Philadelphia, Pennsylvania, Elsevier/Mosby Inc., 2008, pp 97–110
31. Wagner PD: Gas exchange, Clinical Respiratory Medicine, 4th Edition. Edited by Spiro SG, Silvestri GA, Agusti A. Philadelphia, Pennsylvania, Elsevier/Saunders, 2012, pp 37–49
32. West JB: Ventilation, Respiratory Physiology – The Essentials, 4th edition. Baltimore, Williams & Wilkins, 1990, pp 17–8
33. Hendrickx J, Peyton PJ, De Wolf AM: Inhaled anaesthetics and N_2O: Complexities overlooked - Things may not be what they seem. Eur J Anaesth 2016; 33:611–9

34. Wagner PD, Laravuso RB, Uhl RR, West JB: Continuous distributions of ventilation-perfusion ratios in normal subjects breathing air and 100 per cent O2. J Clin Invest 1974; 54:54–68
35. Wagner PD, Laravuso RB, Goldzimmer E, Naumann PF, West JB: Distribution of ventilation-perfusion ratios in dogs with normal and abnormal lungs. J Appl Physiol 1975; 38:1099–109
36. Scheid P, Piiper J: Intrapulmonary gas mixing and stratification, Pulmonary Gas Exchange. Edited by West JB. New York, Academic Press Publishers, 1980, pp 87–130
37. Piiper J, Scheid P: Blood gas equilibration in the lung, Pulmonary Gas Exchange. Edited by West JB. New York, Academic Press Publishers, 1980, pp 131–71